

Digital and Hybrid Precoding Designs in Massive MIMO with Low-Resolution ADCs

Mengyuan Ma, *Student Member, IEEE*, Nhan Thanh Nguyen, *Member, IEEE*,

Italo Atzeni, *Senior Member, IEEE*, A. Lee Swindlehurst, *Fellow, IEEE*, and Markku Juntti, *Fellow, IEEE*

Abstract—Low-resolution analog-to-digital converters (ADCs) have emerged as an efficient solution for massive multiple-input multiple-output (MIMO) systems to reap high data rates with reasonable power consumption and hardware complexity. In this paper, we study precoding designs for digital, fully connected (FC) hybrid, and partially connected (PC) hybrid beamforming architectures in massive MIMO systems with low-resolution ADCs at the receiver. We aim to maximize the spectral efficiency (SE) subject to a transmit power budget and hardware constraints on the analog components. The resulting problems are nonconvex and the quantization distortion introduces additional challenges. To address them, we first derive a tight lower bound for the SE, based on which we optimize the precoders for the three beamforming architectures under the majorization-minimization framework. Numerical results validate the superiority of the proposed precoding designs over their state-of-the-art counterparts in systems with low-resolution ADCs, particularly those with 1-bit resolution. The results show that the PC hybrid precoding design can achieve an SE close to those of the digital and FC hybrid precoding designs in 1-bit systems, highlighting the potential of the PC hybrid beamforming architectures.

Index Terms—Digital precoding, hybrid precoding, low-resolution ADCs, massive MIMO.

I. INTRODUCTION

Massive multiple-input multiple-output (MIMO) technology is crucial for wireless communications at both sub-6 GHz and millimeter wave (mmWave) frequencies, addressing the increasing demand for high data rates [1]. The large number of antenna elements and the use of beamforming techniques significantly improve the spatial multiplexing gain and enable a high spectral efficiency (SE). However, a large number of power-hungry radio-frequency (RF) chains would cause high power consumption, degrading the system's energy efficiency. In this respect, analog-to-digital converters (ADCs) are the most power-consuming RF components at the receiver, as their power consumption increases exponentially with the number of resolution bits [2]. Therefore, using low-resolution ADCs is considered to be an effective approach to reduce the power consumption without excessively compromising the SE performance [3]. However, the non-linear quantization distortion introduces additional challenges, calling for more efficient beamforming designs for achieving a satisfactory SE.

Existing precoding algorithms (e.g., [4]–[7]) are mainly designed for digital beamforming (DBF) and hybrid beamforming (HBF) architectures. DBF architectures require a dedicated RF chain for each antenna, providing large spatial multiplexing gains at the expense of high power consumption. In contrast, HBF architectures employ fewer RF chains with a network of analog components, such as phase-shifters, to cut the hardware power consumption and cost at the expense of reduced spatial multiplexing. HBF implementations can be further divided into fully connected (FC) and partially connected (PC) HBF architectures (FC-HBF and PC-HBF). In the former, each RF chain can access all the antenna elements, while in the latter only a subset of the antenna elements is connected to each RF chain.

Traditional FC and PC hybrid precoding designs [4]–[7] have predominantly focused on full-resolution systems, i.e., with high-resolution ADCs at the receiver. However, these designs tend to underperform in systems with low-resolution ADCs since they do not take the quantization distortion at the receiver into account. To address this challenge, existing studies [8]–[11] have employed a heuristic two-step approach in which the analog precoder is optimized first and the digital precoder is determined second based on the analog design. For instance, Mo *et. al.* [8] derived the analog precoder based on the singular vectors of the channel, followed by the water-filling (WF) method to optimize the digital part. In [9], the analog precoder was chosen from a predefined codebook, after which the digital precoder was optimized to maximize the energy efficiency. Beyond HBF architectures, the quantization distortion also presents challenges for the digital precoding design. Conventional precoding strategies, including zero forcing, maximum ratio transmission, and minimum mean squared error, were explored in [12]–[14]. In [15], we jointly optimized the digital precoder and combiner, resulting in a substantial SE improvement over traditional WF solutions.

Despite the advances discussed above [8]–[15], most studies have focused on only one of the three beamforming architectures: DBF, FC-HBF, or PC-HBF. Furthermore, HBF studies have often relied on heuristic methods for the analog precoding design, leaving considerable room for improving the SE. To fill this gap, we herein introduce a novel methodology that directly maximizes the SE and propose precoding designs for all the three architectures in systems with low-resolution ADCs at the receiver. Given the challenges posed by the hardware constraints at the transmitter and the quantization distortion at the receiver, we first derive a tight lower bound for the SE and then propose an iterative algorithm based on the majorization-

This work was supported by the Research Council of Finland (332362 EERA, 336449 Profi6, 346208 6G Flagship, 348396 HIGH-6G, and 357504 EETCAMD) and by the U.S. National Science Foundation (CCF-2225575). M. Ma, N. T. Nguyen, I. Atzeni, and M. Juntti are with the Centre for Wireless Communications, University of Oulu, Finland (e-mail: {mengyuan.ma, nhan.nguyen, italo.atzeni, markku.juntti}@oulu.fi). A. L. Swindlehurst is with the Center for Pervasive Communications & Computing, University of California, Irvine, CA, USA (email: swindle@uci.edu).

minimization (MM) framework to optimize the precoders. Building on this, we develop efficient precoding designs for the DBF, FC-HBF, and PC-HBF architectures. Numerical results demonstrate that the proposed precoding designs outperform state-of-the-art methods [4], [6], [8], [15] in systems with low-resolution ADCs, particularly those with 1-bit resolution. Notably, our results indicate that the PC hybrid precoding design can achieve an SE close to those of the digital and FC hybrid precoding designs in 1-bit systems, highlighting the potential of PC-HBF architectures.

II. SYSTEM AND QUANTIZATION MODELS

A. MIMO Architecture Models

We consider a point-to-point narrowband MIMO system where a transmitter (Tx) with N_t antennas sends signals to a digital receiver (Rx) with N_r antennas, where the latter employs low-resolution ADCs. Let $\mathbf{s} \in \mathbb{C}^{N_s} \sim \mathcal{CN}(0, \mathbf{I})$ denote the transmitted signal vector and let $\mathbf{F} \in \mathbb{C}^{N_t \times N_s}$ be the precoding matrix with power constraint $\|\mathbf{F}\|_F^2 \leq P_t$, where P_t denotes the transmit power budget and $\|\cdot\|_F$ represents the Frobenius norm. For HBF architectures, \mathbf{F} is given by $\mathbf{F} = \mathbf{F}_{\text{RF}}\mathbf{F}_{\text{BB}}$, where $\mathbf{F}_{\text{RF}} \in \mathbb{C}^{N_t \times N_{\text{RF}}}$ and $\mathbf{F}_{\text{BB}} \in \mathbb{C}^{N_{\text{RF}} \times N_s}$ are the analog and digital precoders, respectively, assuming N_{RF} RF chains ($N_s \leq N_{\text{RF}} \ll N_t$). Each RF chain in the FC-HBF architecture is connected to all antennas through a network of phase shifters, while each RF chain in the PC-HBF architecture is connected only to a set of $M = \frac{N_t}{N_{\text{RF}}}$ antennas. For simplicity, we assume that M is an integer and the N_{RF} groups of antennas are non-overlapping. Let $\mathcal{F}_{\text{full}}$ and \mathcal{F}_{sub} denote the sets of feasible analog precoders for the FC-HBF and PC-HBF architectures, respectively, which can be expressed as

$$\mathcal{F}_{\text{full}} = \{\mathbf{F}_{\text{RF}} : |\mathbf{F}_{\text{RF}}(i, j)| = 1, \forall i, j\}, \quad (1)$$

$$\mathcal{F}_{\text{sub}} = \{\mathbf{F}_{\text{RF}} : \mathbf{F}_{\text{RF}} = \text{blkdiag}(\mathbf{f}_1, \dots, \mathbf{f}_{N_{\text{RF}}}), \\ \mathbf{f}_n \in \mathbb{C}^M, |\mathbf{f}_n(i)| = 1, \forall n, i\}, \quad (2)$$

where $\mathbf{A}(i, j)$ and $\mathbf{a}(i)$ denote the (i, j) -th entry of \mathbf{A} and the i -th element of \mathbf{a} , respectively.

Let $\mathbf{H} \in \mathbb{C}^{N_r \times N_t}$ be the channel between the Tx and Rx. The received signal can be expressed as

$$\mathbf{y} = \mathbf{H}\mathbf{F}\mathbf{s} + \mathbf{n}, \quad (3)$$

where $\mathbf{n} \sim \mathcal{CN}(0, \sigma_n^2 \mathbf{I})$ denotes an additive white Gaussian noise (AWGN) vector with power σ_n^2 . We assume that \mathbf{H} is constant during each coherence time. In order to characterize the performance upper bound under our proposed scheme, we assume the availability of perfect channel state information at both the Tx and Rx [4]–[15]. The quantization model is detailed next.

B. Signal Model with Quantization

Assume that the ADCs are Lloyd-Max quantizers [16] and that the Rx employs two identical ADCs in each RF chain to separately quantize the in-phase and quadrature signals. The codebook for a scalar quantizer of b bits is defined as $\mathcal{C} = \{c_0, \dots, c_{N_q-1}\}$, where $N_q = 2^b$ is the number of output

levels of the quantizer. The set of quantization thresholds is $\mathcal{T} = \{t_0, \dots, t_{N_q}\}$, where $t_0 = -\infty$ and $t_{N_q} = \infty$ allow inputs with arbitrary power. Let $Q(\cdot)$ denote the quantization function. For a complex signal $x = \Re\{x\} + j\Im\{x\}$, we have $Q(x) = Q(\Re\{x\}) + jQ(\Im\{x\})$, with $Q(\Re\{x\}) = c_i$ when $\Re\{x\} \in [t_i, t_{i+1}]$; the imaginary term $Q(\Im\{x\})$ is obtained similarly. When the quantizer input is a vector, $Q(\cdot)$ is applied element-wise.

With fixed \mathbf{H} and \mathbf{F} , we have $\mathbf{y} \sim \mathcal{CN}(0, \mathbf{C}_y)$, where \mathbf{C}_y is the covariance matrix of \mathbf{y} , given by

$$\mathbf{C}_y = \mathbb{E}[\mathbf{y}\mathbf{y}^H] = \mathbf{H}\mathbf{F}\mathbf{F}^H\mathbf{H}^H + \sigma_n^2 \mathbf{I}. \quad (4)$$

Let $\mathbf{z} = Q(\mathbf{y})$ be the quantization of \mathbf{y} . Using the Bussgang decomposition [17], we can write

$$\mathbf{z} = \mathbf{G}\mathbf{y} + \boldsymbol{\eta}, \quad (5)$$

where \mathbf{G} and $\boldsymbol{\eta}$ represent the Bussgang gain matrix and the quantization distortion vector, respectively. Furthermore, \mathbf{G} can be expressed as $\mathbf{G} = \mathbf{I} - \boldsymbol{\Gamma}$, with $\boldsymbol{\Gamma} = \text{diag}(\gamma_1, \dots, \gamma_{N_r})$. Here, γ_i denotes the distortion factor of the ADCs for the i -th RF chain, which depends on the number of resolution bits as $\gamma(b) \approx 2^{-1.74b+0.28}$ [15]. Combined with (3), (5) can be rewritten as

$$\mathbf{z} = \mathbf{G}\mathbf{H}\mathbf{F}\mathbf{s} + \mathbf{e}, \quad (6)$$

where $\mathbf{e} = \mathbf{G}\mathbf{n} + \boldsymbol{\eta}$ represents the effective noise, which is not Gaussian due to the non-linear quantization distortion.

III. DIGITAL AND HYBRID PRECODING DESIGNS

A. Problem Formulation

Treating the effective noise \mathbf{e} as Gaussian, we can obtain a lower bound for the SE as [8], [15]

$$R = \log \det(\mathbf{I} + \mathbf{C}_e^{-1} \mathbf{G}\mathbf{H}\mathbf{F}\mathbf{F}^H\mathbf{H}^H\mathbf{G}), \quad (7)$$

where the covariance matrix of \mathbf{e} is given by $\mathbf{C}_e = \mathbb{E}[\mathbf{e}\mathbf{e}^H] = \mathbf{C}_\eta + \sigma_n^2 \mathbf{G}^2$. Here, $\mathbf{C}_\eta = \mathbb{E}[\boldsymbol{\eta}\boldsymbol{\eta}^H]$ is the covariance of the quantization distortion, which can be approximated as $\mathbf{C}_\eta \approx \mathbf{G}(\mathbf{I} - \mathbf{G})\text{diag}(\mathbf{C}_y)$ [15]. Thus, we obtain

$$\mathbf{C}_e \approx \mathbf{G}(\mathbf{I} - \mathbf{G})\text{diag}(\mathbf{H}\mathbf{F}\mathbf{F}^H\mathbf{H}^H) + \sigma_n^2 \mathbf{G}. \quad (8)$$

We are interested in optimizing the precoder \mathbf{F} to maximize the SE in (7), i.e.,

$$\underset{\|\mathbf{F}\|_F^2 \leq P_t}{\text{maximize}} R(\mathbf{F}). \quad (9)$$

For HBF architectures, the additional constraints

$$\mathbf{F} = \mathbf{F}_{\text{RF}}\mathbf{F}_{\text{BB}}, \quad (10)$$

$$\mathbf{F}_{\text{RF}} \in \mathcal{F} \quad (11)$$

must be satisfied, where $\mathcal{F} = \mathcal{F}_{\text{full}}$ for FC-HBF and $\mathcal{F} = \mathcal{F}_{\text{sub}}$ for PC-HBF. Problem (9) is nonconvex and more challenging compared with conventional precoding designs in full-resolution systems because \mathbf{C}_e depends on \mathbf{F} through (8). To overcome this difficulty, we propose an efficient iterative algorithm based on the MM framework. To make the problem more tractable, we first derive a tight lower bound for $R(\mathbf{F})$ in the following lemma.

Lemma 1 Let $\hat{\mathbf{F}}$ be a prior estimate of \mathbf{F} and define $\mathbf{X} = \mathbf{G}\mathbf{H}\mathbf{F}$. Furthermore, let

$$g(\mathbf{F}, \hat{\mathbf{F}}) = R(\hat{\mathbf{F}}) - \text{Tr}(\hat{\mathbf{X}}^{\text{H}}\hat{\mathbf{C}}_e^{-1}\hat{\mathbf{X}}) + 2\Re\{\text{Tr}(\hat{\mathbf{X}}^{\text{H}}\hat{\mathbf{C}}_e^{-1}\mathbf{X})\} - \text{Tr}\{\hat{\mathbf{S}}(\mathbf{C}_e + \mathbf{X}\mathbf{X}^{\text{H}})\}, \quad (12)$$

where $\hat{\mathbf{X}}$ and $\hat{\mathbf{C}}_e$ are obtained based on $\hat{\mathbf{F}}$, and $\hat{\mathbf{S}} = \hat{\mathbf{C}}_e^{-1} - (\hat{\mathbf{C}}_e + \hat{\mathbf{X}}\hat{\mathbf{X}}^{\text{H}})^{-1}$. Note that $g(\mathbf{F}, \hat{\mathbf{F}})$ depends on \mathbf{F} and $\hat{\mathbf{F}}$ through $\{\mathbf{X}, \mathbf{C}_e\}$ and $\{\hat{\mathbf{X}}, \hat{\mathbf{C}}_e\}$, respectively. It can be shown that $g(\mathbf{F}, \hat{\mathbf{F}})$ is a tight lower bound for $R(\mathbf{F})$, i.e., $g(\mathbf{F}, \hat{\mathbf{F}}) \leq R(\mathbf{F})$, where the equality holds only if $\hat{\mathbf{F}} = \mathbf{F}$.

Lemma 1 is obtained based on [18, Proposition 7]; the proof is omitted due to space limitations. Using Lemma 1, we can update \mathbf{F} by iteratively maximizing $g(\mathbf{F}, \hat{\mathbf{F}})$ using the MM framework. Next, we use this method to propose efficient solutions for digital and hybrid precoding.

B. Digital Precoding Design

Let p_i^2 be the power allocated to the i -th data stream, and let $\mathbf{p} = [p_1, \dots, p_{N_s}]^{\text{T}}$. Furthermore, let $\mathbf{H} = \mathbf{U}\Sigma\mathbf{V}^{\text{H}}$ be the singular value decomposition (SVD) of \mathbf{H} . The precoder can be constructed as

$$\mathbf{F} = \tilde{\mathbf{V}}\text{diag}(\mathbf{p}), \quad (13)$$

where $\tilde{\mathbf{V}} = \mathbf{V}(:, 1 : N_s)$ contains the N_s right-singular vectors associated with the N_s largest singular values of \mathbf{H} . As a result, the precoding design becomes the power allocation problem $\text{maximize}_{\|\mathbf{p}\|_2^2 \leq P_t} g(\mathbf{p}, \hat{\mathbf{p}})$ that follows from Lemma 1. After some algebraic manipulations, we obtain the equivalent problem

$$\text{minimize}_{\mathbf{p}} \sum_{i=1}^{N_s} \hat{\mathbf{J}}(i, i)p_i^2 - 2 \sum_{i=1}^{N_s} \Re\{\hat{\mathbf{K}}(i, i)p_i\} \quad (14a)$$

$$\text{s.t.} \quad \sum_{i=1}^{N_s} p_i^2 \leq P_t, \quad (14b)$$

where $\hat{\mathbf{J}} = \tilde{\mathbf{V}}^{\text{H}}\mathbf{H}^{\text{H}}(\mathbf{G}\hat{\mathbf{S}}\mathbf{G} + \text{diag}(\hat{\mathbf{S}})\mathbf{G}(\mathbf{I} - \mathbf{G}))\mathbf{H}\tilde{\mathbf{V}}$, $\hat{\mathbf{K}} = \text{diag}(\hat{\mathbf{p}}^{\frac{1}{2}})\tilde{\mathbf{V}}^{\text{H}}\mathbf{H}^{\text{H}}\mathbf{G}\hat{\mathbf{C}}_e^{-1}\mathbf{G}\mathbf{H}\tilde{\mathbf{V}}\text{diag}(\hat{\mathbf{p}}^{\frac{1}{2}})$, and $\hat{\mathbf{a}}^{\frac{1}{2}}$ is obtained by taking the element-wise square root of the elements of \mathbf{a} . Setting the derivative of the Lagrangian of (14) to zero, we obtain the solution as

$$p_i = \frac{\hat{\mathbf{K}}(i, i)}{\hat{\mathbf{J}}(i, i) + \mu} \quad \forall i, \quad (15)$$

where μ is the associated Lagrange multiplier, which can be obtained via a bisection search over $(0, \mu_{\text{ub}}]$ to satisfy $\sum_{i=1}^{N_s} p_i^2 = P_t$, where $\mu_{\text{ub}} = \frac{1}{\sqrt{P_t}} \|\text{diag}(\hat{\mathbf{K}})\|_{\text{F}}$ is obtained by letting $\hat{\mathbf{J}} = \mathbf{0}$.

The proposed digital precoding design is summarized in Algorithm 1. We note that the conventional WF solution, denoted by \mathbf{F}_{WF} , is obtained by assuming $\mathbf{C}_{\eta} = \mathbf{0}$ as in full-resolution systems. Hence, \mathbf{F}_{WF} is sub-optimal for (14) due to the presence of the quantization distortion, as will be shown in Section IV.

C. Hybrid Precoding Design

Define $f(\mathbf{F}_{\text{RF}}, \mathbf{F}_{\text{BB}}) = \text{Tr}(\hat{\mathbf{L}}\mathbf{F}_{\text{RF}}\mathbf{F}_{\text{BB}}\mathbf{F}_{\text{BB}}^{\text{H}}\mathbf{F}_{\text{RF}}^{\text{H}}) - 2\Re\{\text{Tr}(\hat{\mathbf{D}}\mathbf{F}_{\text{RF}}\mathbf{F}_{\text{BB}})\}$ with $\hat{\mathbf{D}} = \hat{\mathbf{X}}^{\text{H}}\hat{\mathbf{C}}_e^{-1}\mathbf{G}\mathbf{H}$ and $\hat{\mathbf{L}} =$

Algorithm 1: MM-based Digital Precoding Design

Output: \mathbf{F}

- 1 Initialize \mathbf{p}, ϵ .
- 2 Perform SVD $\mathbf{H} = \mathbf{U}\Sigma\mathbf{V}^{\text{H}}$ and set $\tilde{\mathbf{V}} = \mathbf{V}(:, 1 : N_s)$.
- 3 **repeat**
- 4 $\hat{\mathbf{p}} \leftarrow \mathbf{p}$.
- 5 Update \mathbf{p} as in (15).
- 6 **until** $|R(\mathbf{p}) - R(\hat{\mathbf{p}})| \leq \epsilon$;
- 7 Obtain \mathbf{F} by (13).

$\mathbf{H}^{\text{H}}(\text{diag}(\hat{\mathbf{S}})\mathbf{G}(\mathbf{I} - \mathbf{G}) + \mathbf{G}\hat{\mathbf{S}}\mathbf{G})\mathbf{H}$. Using Lemma 1, the subproblem for the hybrid precoding design in each iteration is expressed as

$$\text{minimize}_{\mathbf{F}, \mathbf{F}_{\text{RF}}, \mathbf{F}_{\text{BB}}} f(\mathbf{F}_{\text{RF}}, \mathbf{F}_{\text{BB}}) \quad (16a)$$

$$\text{s.t.} \quad (10) \text{ and } (11),$$

$$\|\mathbf{F}\|_{\text{F}}^2 \leq P_t, \quad (16b)$$

which is challenging due to the constraints (10) and (11). Observing that $f(\mathbf{F}_{\text{RF}}, \mathbf{F}_{\text{BB}})$ is convex with respect to \mathbf{F}_{RF} (\mathbf{F}_{BB}) when \mathbf{F}_{BB} (\mathbf{F}_{RF}) is fixed, we compute the analog and digital precoders via alternating optimization, as explained next.

1) *Update \mathbf{F}_{RF}* : For a given \mathbf{F}_{BB} , the problem of designing \mathbf{F}_{RF} can be written as $\text{minimize}_{\mathbf{F}_{\text{RF}} \in \mathcal{F}} f(\mathbf{F}_{\text{RF}}, \mathbf{F}_{\text{BB}})$, with $\mathcal{F} = \mathcal{F}_{\text{full}}$ for FC-HBF and $\mathcal{F} = \mathcal{F}_{\text{sub}}$ for PC-HBF. To efficiently solve this problem, we propose to use the projected gradient descent (PGD) method. Specifically, let $\nabla_{\mathbf{F}_{\text{RF}}} f$ denote the gradient of $f(\mathbf{F}_{\text{RF}}, \mathbf{F}_{\text{BB}})$ with respect to \mathbf{F}_{RF} , given by

$$\nabla_{\mathbf{F}_{\text{RF}}} f = 2(\hat{\mathbf{L}}\mathbf{F}_{\text{RF}}\mathbf{F}_{\text{BB}} - \hat{\mathbf{D}}^{\text{H}})\mathbf{F}_{\text{BB}}^{\text{H}}, \quad (17)$$

and let $\text{Proj}_{\mathcal{F}}(\mathbf{F}_{\text{RF}})$ represent the operation that projects \mathbf{F}_{RF} onto \mathcal{F} . Define $\mathbf{W} = \text{blkdiag}(\mathbf{1}_M, \dots, \mathbf{1}_M)$, where $\mathbf{1}_M \in \mathbb{R}^M$ is the M -dimensional all-one vector. The projectors for FC-HBF and PC-HBF are given by

$$\text{Proj}_{\mathcal{F}_{\text{full}}}(\mathbf{F}_{\text{RF}}) = e^{j\angle\mathbf{F}_{\text{RF}}}, \quad (18a)$$

$$\text{Proj}_{\mathcal{F}_{\text{sub}}}(\mathbf{F}_{\text{RF}}) = \mathbf{W} \odot e^{j\angle\mathbf{F}_{\text{RF}}}, \quad (18b)$$

respectively, where $\angle\mathbf{F}_{\text{RF}}$ returns the angles of each entry of \mathbf{F}_{RF} and \odot denotes the Hadamard product. The update rules for the PGD method can be expressed as

$$\mathbf{F}_{\text{RF}} \leftarrow \text{Proj}_{\mathcal{F}} \left(\tilde{\mathbf{F}}_{\text{RF}} - \beta \frac{\nabla_{\mathbf{F}_{\text{RF}}} f}{\|\nabla_{\mathbf{F}_{\text{RF}}} f\|_{\text{F}}} \Big|_{\mathbf{F}_{\text{RF}} = \tilde{\mathbf{F}}_{\text{RF}}} \right), \quad (19)$$

where β denotes the step size and $\tilde{\mathbf{F}}_{\text{RF}}$ is the iterate of \mathbf{F}_{RF} . The detailed steps for obtaining \mathbf{F}_{RF} are similar to those in [19, Algorithm 1] and are thus omitted.

2) *Update \mathbf{F}_{BB}* : For a given \mathbf{F}_{RF} , we can obtain a closed-form solution for \mathbf{F}_{BB} as

$$\mathbf{F}_{\text{BB}} = (\mathbf{F}_{\text{RF}}^{\text{H}}\hat{\mathbf{L}}\mathbf{F}_{\text{RF}} + \lambda\mathbf{F}_{\text{RF}}^{\text{H}}\mathbf{F}_{\text{RF}})^{-1}\mathbf{F}_{\text{RF}}^{\text{H}}\hat{\mathbf{D}}^{\text{H}}, \quad (20)$$

where λ is the Lagrange multiplier associated with the power constrain, and can be obtained via a bisection search over $(0, \lambda_{\text{ub}}]$, with $\lambda_{\text{ub}} = \frac{1}{\sqrt{P_t}} \|(\mathbf{F}_{\text{RF}}^{\text{H}}\mathbf{F}_{\text{RF}})^{-\frac{1}{2}}\mathbf{F}_{\text{RF}}^{\text{H}}\hat{\mathbf{D}}^{\text{H}}\|_{\text{F}}$, based on the complementary slackness condition $\lambda(\text{Tr}(\mathbf{F}_{\text{RF}}^{\text{H}}\mathbf{F}_{\text{RF}}\mathbf{F}_{\text{BB}}\mathbf{F}_{\text{BB}}^{\text{H}}) - P_t) = 0$.

The proposed hybrid precoding design is summarized in

Algorithm 2: MM-based Hybrid Precoding Design

Output: $\mathbf{F}_{\text{RF}}, \mathbf{F}_{\text{BB}}$
1 Initialize $\mathbf{F}_{\text{RF}} \in \mathcal{F}, \mathbf{F}, \mathbf{F}_{\text{BB}} = \mathbf{F}_{\text{RF}}^\dagger \mathbf{F}, \epsilon$.
2 **repeat**
3 $\hat{\mathbf{F}} \leftarrow \mathbf{F}$.
4 **repeat**
5 Update \mathbf{F}_{RF} via the PGD method.
6 Update \mathbf{F}_{BB} as in (20).
7 **until** $f(\mathbf{F}_{\text{RF}}, \mathbf{F}_{\text{BB}})$ stops decreasing;
8 $\mathbf{F} = \mathbf{F}_{\text{RF}} \mathbf{F}_{\text{BB}}$.
9 **until** $|R(\mathbf{F}) - R(\hat{\mathbf{F}})| \leq \epsilon$;

Algorithm 2. The precoder \mathbf{F} is initialized with the conventional WF precoder \mathbf{F}_{WF} . Let $\mathbf{V}_a = \mathbf{V}(:, 1 : N_{\text{RF}})$ contain the N_{RF} singular vectors associated with the N_{RF} largest singular values of \mathbf{H} . We initialize $\mathbf{F}_{\text{RF}} = \mathbf{V}_a$ for FC-HBF or $\mathbf{F}_{\text{RF}} = \mathbf{W} \odot \mathbf{V}_a$ for PC-HBF, which yields $\mathbf{F}_{\text{BB}} = \mathbf{F}_{\text{RF}}^\dagger \mathbf{F}_{\text{WF}}$. Algorithms 1 and 2 are guaranteed to converge according to the MM theory.

D. Complexity Analysis

Let I_1 be the number of iterations for Algorithm 1. With $N_s \ll \min(N_r, N_t)$, the complexity of Algorithm 1 can be expressed as $I_1 \mathcal{O}(2N_r^2 N_t + 2N_r^3 + 4N_r^2 N_s + 6N_r N_t N_s)$ floating-point operations (FLOPs) due mainly to matrix multiplications and inverses. For Algorithm 2, step 5 has a complexity of $\mathcal{O}(I_{\text{pgd}} N_t^2 N_{\text{RF}})$ due to the matrix multiplication, where I_{pgd} denotes the number of PGD iterations, whereas computing \mathbf{F}_{BB} in step 6 requires $\mathcal{O}(N_t^2 N_{\text{RF}})$ FLOPs. Furthermore, $\hat{\mathbf{X}}, \hat{\mathbf{C}}_e, \hat{\mathbf{L}},$ and $\hat{\mathbf{D}}$ are computed in the outer loop, requiring $\mathcal{O}(2N_r^2 N_t + 2N_r^3 + 6N_r^2 N_{\text{RF}} + 5N_r N_t N_{\text{RF}})$ FLOPs. Therefore, the complexity of Algorithm 2 can be expressed as $I_{\text{out}} N_{\text{RF}} \mathcal{O}(6N_r^2 + 5N_r N_t + I_{\text{in}} I_{\text{pgd}} N_t^2) + I_{\text{out}} \mathcal{O}(2N_r^2 N_t + 2N_r^3)$, where I_{in} and I_{out} denote, respectively, the number of iterations for the inner and outer loops of Algorithm 2.

The complexity of the proposed algorithms is summarized and compared with that in [4], [6], [8], [15] in Table I. Algorithm 1 has a lower complexity than the digital precoding design in [15], as the former focuses only on precoding. Algorithm 2 has a higher complexity compared with the algorithms in [4], [6], [8] due to the optimization of the hybrid precoders to directly maximize the SE. However, the proposed digital precoding design can achieve an SE comparable to that of [15], and the proposed hybrid precoding designs can attain higher SE in low-resolution systems, as illustrated next.

IV. NUMERICAL RESULTS

In all simulations, we assume that the system operates at 28 GHz with bandwidth of 1 GHz. We employ the Saleh-Valenzuela channel model and configure the channel parameters as those in [4]. The signal-to-noise ratio (SNR) is defined as $\text{SNR} = \frac{P_t}{\sigma_n^2}$ and we assume identical b -bit ADCs for each RF chain. The other parameters are detailed in the caption of each figure. All the results are obtained by averaging over 10^3 independent channel realizations.

For comparison, we consider the following baselines:

Algorithm	Computational complexity
Algorithm 1	$I_1 \mathcal{O}(2N_r^2 N_t + 2N_r^3 + 4N_r^2 N_s + 6N_r N_t N_s)$
DBF [15]	$I_n \mathcal{O}(3N_t^3 + 3N_t^2 + 8N_t^2 N_r + 8N_t N_r^2)$
Algorithm 2	$I_{\text{out}} N_{\text{RF}} \mathcal{O}(6N_r^2 + 5N_r N_t + I_{\text{in}} I_{\text{pgd}} N_t^2) + I_{\text{out}} \mathcal{O}(2N_r^2 N_t + 2N_r^3)$
FC-HBF [8]	$\mathcal{O}(N_t N_r N_{\text{RF}} + I_c N_t N_{\text{RF}}^2 + 2I_c N_{\text{RF}}^3)$
FC-HBF [4]	$I_o \mathcal{O}(2N_t N_{\text{RF}}^2 + I_i N_t^2 N_{\text{RF}})$
PC-HBF [6]	$\mathcal{O}(N_r^3 N_{\text{RF}} + N_r^2 N_t N_{\text{RF}} + N_t^2 N_r N_{\text{RF}})$

TABLE I. Computational complexity of the considered algorithms. Here, I_n and I_c denote the number of iterations of the designs in [15] and [8], respectively, while I_o and I_i represent the number of iterations of the outer and inner loop for the method in [4].

- “UqOpt”: Using \mathbf{F}_{WF} for maximizing the SE with full-resolution ADCs.
- “DBF: WF”: Using \mathbf{F}_{WF} with low-resolution ADCs.
- “DBF: JPC”: Joint design of digital precoder and combiner for low-resolution ADCs [15].
- “FC-HBF: SVD-based”: SVD-based FC hybrid precoding with low-resolution ADCs [8].
- “FC-HBF: AO”: FC hybrid precoding design with full-resolution systems [4].
- “PC-HBF: SVD-based”: Modified SVD-based design [8] with projection of the analog precoder onto \mathcal{F}_{sub} .
- “PC-HBF: SIC”: PC hybrid precoding design with full-resolution systems [6].

Additionally, the SE of all the precoding schemes is based on the simulated \mathbf{C}_η for a more practical performance characterization (rather than on the diagonal approximation in (8)). The simulated \mathbf{C}_η is obtained using a sample average over 10^5 realizations.

In Figs. 1(a) and 1(b), we plot the SE versus the SNR and ADC resolution, respectively, with $N_t = N_r = 64$ and $N_s = N_{\text{RF}} = 8$. From Fig. 1(a), we observe that the proposed digital precoding design achieves an SE comparable to that of the “DBF: JPC”. Furthermore, the proposed FC-HBF and PC-HBF schemes outperform their benchmark counterparts and perform better at high SNR. For example, at SNR = 20 dB, the proposed FC-HBF and PC-HBF approaches achieve 19% and 21% improvements in SE over the “FC-HBF: AO” and “PC-HBF: SVD-based”, respectively. Additionally, it is seen that both the proposed FC and PC hybrid precoding designs outperform WF-based digital precoding in low-resolution systems at high SNR. In particular, the proposed FC hybrid precoding design attains SE comparable to that of the proposed digital one. Fig. 1(b) shows that the proposed DBF, FC-HBF, and PC-HBF schemes achieve significantly higher SE compared with their benchmarks, especially for low ADC resolutions. Notably, PC-HBF achieves an SE comparable to those of DBF and FC-HBF as the ADC resolution decreases. This is further illustrated in Fig. 1(c), which shows the SE gain in % of DBF, FC-HBF, and PC-HBF compared with the WF-based digital precoding design. The proposed precoding designs achieve 51%, 51%, and 49% SE gains with 1-bit ADCs. However, when $b \geq 8$, PC-HBF achieves lower SE than WF-based DBF.

In Fig. 2, we plot the SE as a function of the number of

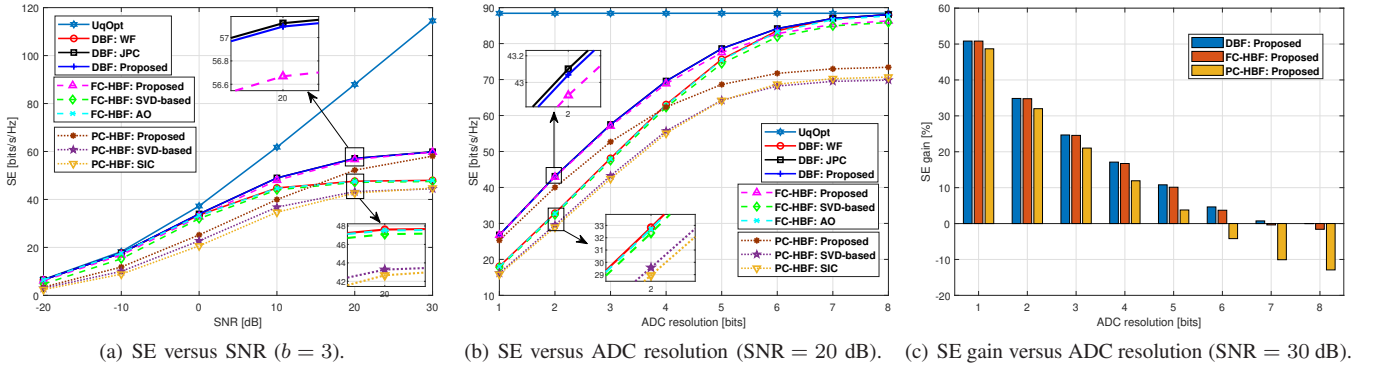


Fig. 1. SE performance ($N_t = N_r = 64$ and $N_s = N_{RF} = 8$).

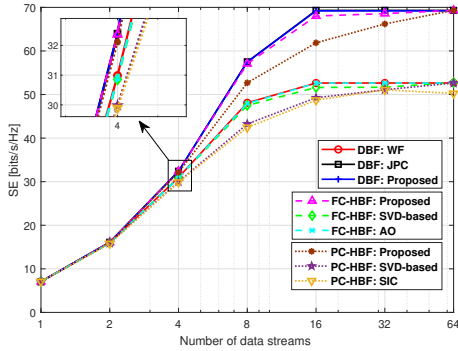


Fig. 2. SE versus number of data streams ($N_r = N_t = 64$, SNR = 20 dB, and $b = 3$).

data streams with $N_r = N_t = 64$, SNR = 20 dB, and $b = 3$. It is seen that the SE gains of the proposed methods are more significant with more data streams. While for $N_s \leq 4$ the SE difference between the proposed precoding design and the benchmark algorithms is relatively small, $N_s \geq 16$ yields a large performance gap. For $N_s = 16$, the proposed precoding designs for the DBF, FC-HBF, and PC-HBF architectures achieve SE gains of 32%, 29%, and 26% compared with the “DBF: WF”, “FC-HBF: AO”, and “PC-HBF: SVD-based”, respectively.

V. CONCLUSIONS

We have investigated precoding designs for DBF, FC-HBF, and PC-HBF architectures in massive MIMO systems with low-resolution ADCs aiming at maximizing the system SE. To solve the resulting challenging nonconvex problem, we first derive a tight lower bound for the SE and then iteratively optimize the precoder under the MM framework. Based on this method, we propose efficient precoding algorithms for DBF, FC-HBF, and PC-HBF architectures. Numerical results demonstrate that the proposed methods significantly outperform the compared benchmarks in low-resolution systems, especially with 1-bit ADCs. Furthermore, the results indicate that the PC hybrid precoding design can achieve SE comparable to those of the digital and FC hybrid precoding designs in 1-bit systems, highlighting the potential of PC-HBF architectures.

REFERENCES

- [1] E. Bjornson, L. Van der Perre, S. Buzzi, and E. G. Larsson, “Massive MIMO in sub-6 GHz and mmWave: Physical, practical, and use-case differences,” *IEEE Wireless Commun.*, vol. 26, no. 2, pp. 100–108, 2019.
- [2] B. Murmann, “The race for the extra decibel: A brief review of current ADC performance trajectories,” *IEEE Solid-State Circuits Mag.*, vol. 7, no. 3, pp. 58–66, 2015.
- [3] I. Atzeni and A. Tölli, “Channel estimation and data detection analysis of massive MIMO with 1-bit ADCs,” *IEEE Trans. Wireless Commun.*, vol. 21, no. 6, pp. 3850–3867, 2022.
- [4] X. Yu, J.-C. Shen, J. Zhang, and K. B. Letaief, “Alternating minimization algorithms for hybrid precoding in millimeter wave MIMO systems,” *IEEE J. Sel. Topics Signal Process.*, vol. 10, no. 3, pp. 485–500, 2016.
- [5] F. Sotriani and W. Yu, “Hybrid digital and analog beamforming design for large-scale antenna arrays,” *IEEE J. Sel. Topics Signal Process.*, vol. 10, no. 3, pp. 501–513, 2016.
- [6] X. Gao, L. Dai, S. Han, I. Chih-Lin, and R. W. Heath, “Energy-efficient hybrid analog and digital precoding for mmWave MIMO systems with large antenna arrays,” *IEEE J. Sel. Areas Commun.*, vol. 34, no. 4, pp. 998–1009, 2016.
- [7] N. T. Nguyen and K. Lee, “Unequally sub-connected architecture for hybrid beamforming in massive MIMO systems,” *IEEE Trans. Wireless Commun.*, vol. 19, no. 2, pp. 1127–1140, 2019.
- [8] J. Mo, A. Alkhateeb, S. Abu-Surra, and R. W. Heath, “Hybrid architectures with few-bit ADC receivers: Achievable rates and energy-rate tradeoffs,” *IEEE Trans. Wireless Commun.*, vol. 16, no. 4, pp. 2274–2287, 2017.
- [9] L.-F. Lin, W.-H. Chung, H.-J. Chen, and T.-S. Lee, “Energy efficient hybrid precoding for multi-user massive MIMO systems using low-resolution ADCs,” in *Proc. IEEE Int. Workshop on Signal Process. Systems.*, 2016.
- [10] X. Qiao, Y. Zhang, M. Zhou, H. Cao, and L. Yang, “Eigen decomposition-based hybrid precoding for millimeter wave MIMO systems with low-resolution ADCs/DACs,” in *Proc. Int. Conf. on Wireless Commun. and Signal Proc.*, 2019.
- [11] Q. Hou, R. Wang, E. Liu, and D. Yan, “Hybrid precoding design for MIMO system with one-bit ADC receivers,” *IEEE Access*, vol. 6, pp. 48 478–48 488, 2018.
- [12] Y. Zhang, D. Li, D. Qiao, and L. Zhang, “Analysis of indoor THz communication systems with finite-bit DACs and ADCs,” *IEEE Trans. Veh. Technol.*, vol. 71, no. 1, pp. 375–390, Jan. 2021.
- [13] O. B. Usman, H. Jedda, A. Mezghani, and J. A. Nossek, “MMSE precoder for massive MIMO using 1-bit quantization,” in *Proc. IEEE Int. Conf. Acoust., Speech, and Signal Process.*, 2016.
- [14] Q. Lin, H. Shen, and C. Zhao, “Learning linear MMSE precoder for uplink massive mimo systems with one-bit ADCs,” *IEEE Wireless Commun. Lett.*, vol. 11, no. 10, pp. 2235–2239, 2022.
- [15] M. Ma, N. T. Nguyen, I. Atzeni, and M. Juntti, “Joint beamforming design and bit allocation in massive MIMO with resolution-adaptive ADCs,” *arXiv preprint arXiv:2407.03796*, 2024.
- [16] J. Max, “Quantizing for minimum distortion,” *IRE Trans. Inf. Theory*, vol. 6, no. 1, pp. 7–12, 1960.
- [17] O. T. Demir and E. Bjornson, “The Busgang decomposition of nonlinear systems: Basic theory and MIMO extensions [lecture notes],” *IEEE Signal Process. Mag.*, vol. 38, no. 1, pp. 131–136, 2020.
- [18] Z. Zhang and Z. Zhao, “Rate maximizations for reconfigurable intelligent surface-aided wireless networks: A unified framework via block minorization-maximization,” *arXiv preprint arXiv:2105.02395*, 2021.
- [19] M. Ma, N. T. Nguyen, I. Atzeni, and M. Juntti, “Hybrid receiver design for massive MIMO-OFDM with low-resolution ADCs and oversampling,” *arXiv preprint arXiv:2407.04408*, 2024.